05

Effect of Vacuum Heat Treatment of $La_{1-x}Sr_xFeO_{3-\delta}$ on Magnetic Hysteresis

© A.I. Dmitriev, M.S. Dmitrieva

Federal Research Center for Problems of Chemical Physics and Medical Chemistry, Russian Academy of Sciences, 142432 Chernogolovka, Moscow region, Russia
e-mail: alex-dmitriev2005@yandex.ru, aid@icp.ac.ru

Received March 28, 2025
Revised April 29, 2025
Accepted May 7, 2025

The dependences of magnetization on the magnetic field strength $M(H)$ in the form of hysteresis loops in a wide temperature range of polycrystalline samples of substituted lanthanum-strontium ferrite $La_{0.67}Sr_{0.33}FeO_{3-\delta}$ before and after vacuum heat treatment were studied in detail. It was found that the microscopic mechanism responsible for the formation of magnetic hysteresis in the original samples is the pinning of domain walls on extended defects, the dimensions of which are smaller than the thickness of the domain wall. In annealed samples, this is the fixation of domain walls on extended defects, the dimensions of which are larger than the thickness of the domain wall.

Keywords: substituted lanthanum-strontium ferrites, magnetic hysteresis.

DOI: 10.61011/TP.2025.11.62234.50-25

Introduction

A number of materials used in modern technologies have a structure of the form ABO_3. The most important of these are perovskites, which are materials with excellent ferroelectric properties and high dielectric constants. The great interest in them is due to the potential wide application in - technology due to the relatively easily changeable properties of the material. The substitution of A or B positions of the perovskite structure ABO_3 allows adjusting the properties to specific applications [1]. Recently, the focus has been on substituted lanthanum-strontium ferrites $La_{1-x}Sc_xFeO_{3-\delta}$ due to -their possible applications in solid oxide fuel cells as cathode materials [2–4], in gas sensors [5], in catalysis [6] and in magnetic data stores, logic devices, sensors [7–9]. These possibilities are attributable to the unique features of rare-earth ferrites with the structure of perovskite [9,10]. Rare-earth ferrites with the general formula $ReFeO_{3-\delta}$ (where Re is a rare-earth element) have a distorted perovskite structure. The orthorhombic structure is formed as a result of the antiphase inclination of neighboring octahedra FeO_6. The cationic sites are easily replaceable, which makes it possible to subtly vary the structure and physical properties of ferrite [10]. This can lead to new unique properties — ferroelectric, magnetic, electrically conductive, piezoelectric, pyroelectric, magneto-optical and others required for specific practical applications [1,11,12]. $LaFeO_{3-\delta}$ is a perovskite material in which the unit cell consists of six ions O^{2-} surrounding the ion Fe^{3+} in octahedral coordination. La^{3+} ions enter the nodes of the octahedron FeO_6 [13]. Deviating from the ideal cubic perovskite, $LaFeO_{3-\delta}$ forms an orthorhombic lattice with ion spins Fe^{3+} directed along the axis a and an antiferromagnetic component, respectively, parallel to the axis a. There is a weak ferromagnetic component along the c axis caused by a small ($\sim 0.5^\circ$) spin deviation from the strict antiparallel [13]. The magnetic properties of $LaFeO_{3-\delta}$ are due only to the ions Fe^{3+}, since the ion La^{3+} is non-magnetic. Accordingly, there is no interaction between the sublattices Fe^{3+} and La^{3+}. Replacement of La^{3+} with Sr^{2+} in substituted lanthanum-strontium ferrite $La_{1-x}Sc_xFeO_{3-\delta}$ leads to significant modification of the structure, as well as magnetic, electronic and catalytic properties. Lattice distortion caused by doping Sr^{2+} can cause changes in the octahedron size FeO_6, bond lengths A–O and B–O, and bond angle Fe–O–Fe. Another consequence of the ion substitution of La^{3+} by Sr^{2+} is an increase in the valence state of Fe ions, since it is trivalent in $LaFeO_{3-\delta}$ and tetravalent in $SrFeO_{3-\delta}$. Thus, replacing La^{3+} with Sr^{2+} to obtain substituted lanthanum-strontium ferrite $La_{1-x}Sc_xFeO_{3-\delta}$ leads to the formation of a mixed valence ion Fe^{3+} and Fe^{4+} in it. The magnetism of mixed-valence compounds is determined by the competition of antiferromagnetic superexchange interactions (J_{AF}) in Fe pairs^{3+}–Fe^{3+} and ferromagnetic exchange interactions (J_F) in pairs Fe^{3+}–Fe^{4+}, proceeding by the double-exchange Zener mechanism [2–13].

In addition to the exchange interaction, the macroscopic manifestation of which is weak ferromagnetism, which occurs in the considered substituted lanthanum-strontium ferrites $La_{1-x}Sc_xFeO_{3-\delta}$ at temperatures below the Neel temperature, the magnetic properties of the latter are controlled by magnetic anisotropy. Its manifestation is magnetic hysteresis. The first phenomenon has been studied in some detail. Very few studies are devoted to the second phenomenon [14–18], and all the mentioned works are descriptive in nature and do not reveal the physics of magnetic hysteresis in substituted lanthanum-strontium ferrite $La_{1-x}Sc_xFeO_{3-\delta}$. Therefore, the aim of

this study was to establish the microscopic mechanisms of the formation of magnetic hysteresis in $La_{1-x}Sc_xFeO_{3-\delta}$ and the effect of vacuum heat treatment on it.

1. Methodology and samples

Polycrystalline samples of substituted lanthanum-strontium ferrite $La_{0.67}Sr_{0.33}FeO_{3-\delta}$ were synthesized at a temperature of 1100°C for 20 h in air by the glycine-nitrate sol-gel method using nitrates Sr, Fe and La as initial reagents in a stoichiometric ratio. The salts and glycine were dissolved in distilled water. The resulting solution was evaporated at a temperature of 250°C. Next, the precursor was ground in an agate mortar, then annealed at a temperature of 800 °C for 5 h. The annealed powder was crushed in a zirconium container of a planetary ball mill with the addition of ethyl alcohol for 3 h. The final annealing of the powders was carried out at a temperature of 1100 °C for 20 h followed by slow cooling together with the furnace. Details of the preparation and certification of samples are given in Ref. [19,20]. Using X-ray diffraction analysis, it was found that the obtained samples have an orthorhombic structure with lattice parameters $a = 5.502$ Å, $b = 5.544$ Å, $c = 7.811$ Å with the inclusion of a certain fraction of the rhombohedral phase. According to scanning electron microscopy data, the samples are conglomerates of sintered particles, the sizes of which depend on annealing (the average size is 0.41 and 0.44 μm before and after vacuum heat treatment, respectively) (Fig. 1). Fe^{3+} and Fe^{4+} ions are present in the samples according to Mossbauer spectroscopy data. After synthesis, some of the initial samples were subjected to vacuum (10^{-3} Torr) heat treatment at 650 °C for 6 h. The annealed series samples have an orthorhombic lattice with $a = 5.535$ Å, $b = 5.548$ Å, $c = 7.838$ Å, practically free of rhombohedral phase admixture, and contain only Fe^{3+} ions. The process occurring during vacuum annealing can be characterized as a change in the local ion environment Fe^{3+} in the direction of reducing its distortion.

The dependences of the magnetic moment on the magnetic field strength $M(H)$ in the form of hysteresis loops over a wide temperature range of the samples before and after vacuum annealing were measured using a vibration magnetometer of the CFMS multifunctional cryomagnetic measuring system from Cryogenic Ltd, UK.

2. Results and their discussion

Fig. 2 shows the dependences of magnetization on the magnetic field strength M(H) in the form of hysteresis loops at different temperatures of polycrystalline samples of substituted lanthanum-strontium ferrite $La_{0.67}Sr_{0.33}FeO_{3-\delta}$ before (Fig. 2, a) and after (Fig. 2, b) vacuum heat treatment. The shape of magnetic hysteresis loops is typical for weak ferromagnets and inherits the shape of the curves $M(H)$ of

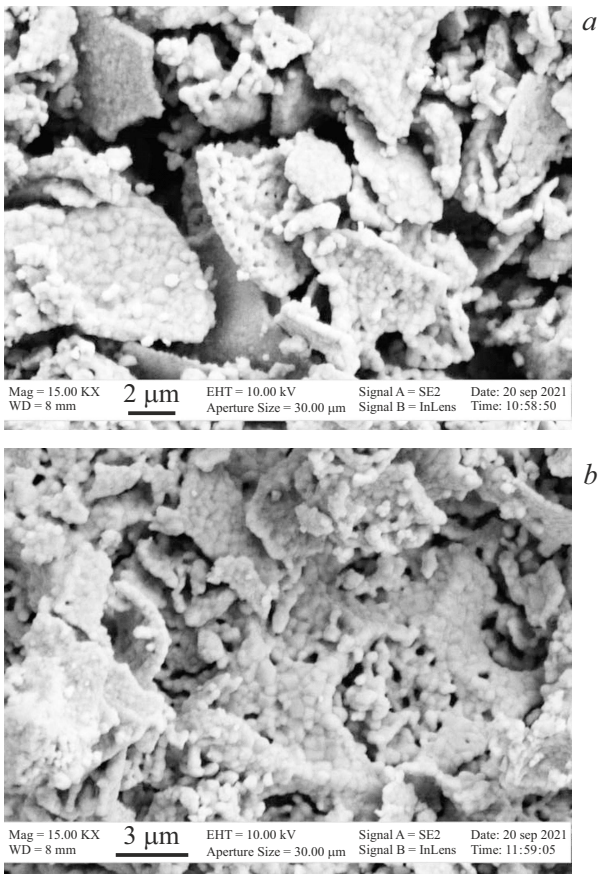

Figure 1. Images obtained by scanning electron microscopy of samples of substituted lanthanum-strontium ferrite $La_{0.67}Sr_{0.33}FeO_{3-\delta}$ before (a) and after (b) vacuum heat treatment.

both antiferromagnets and ferromagnets. The antiferromagnetic component is manifested in relatively strong magnetic fields, the intensity of which exceeds 20 kOe. Here the dependence $M(H)$ is linear. The ferromagnetic component is manifested in relatively weak magnetic fields, the intensity of which is less than 20 kOe. It shows a fairly significant hysteresis and a tendency to saturation. The coercive force H_C in the initial samples reaches 10 kOe at a temperature of $T = 2$ K. Vacuum heat treatment causes an almost twofold decrease in the coercive force, so that it does not reach even 5 kOe at a temperature of $T = 2$ K in annealed samples H_C. In both cases, an increase in temperature leads to a narrowing of the loop. The temperature dependences of the coercive force $H_C(T)$ before and after vacuum heat treatment are shown in Fig. 3. It should be noted that we have not been able to describe the curves $H_C(T)$ with any known empirical expression. We have considered the following cases:

1. Inversely proportional temperature dependence $H_C(T) \sim 1/T$, previously observed, for example, in epitaxial films of Fe/Cu(001) [21]. The mechanisms leading to such dependence were first considered by Egami. In highly anisotropic ferromagnets, the Bloch wall is exposed

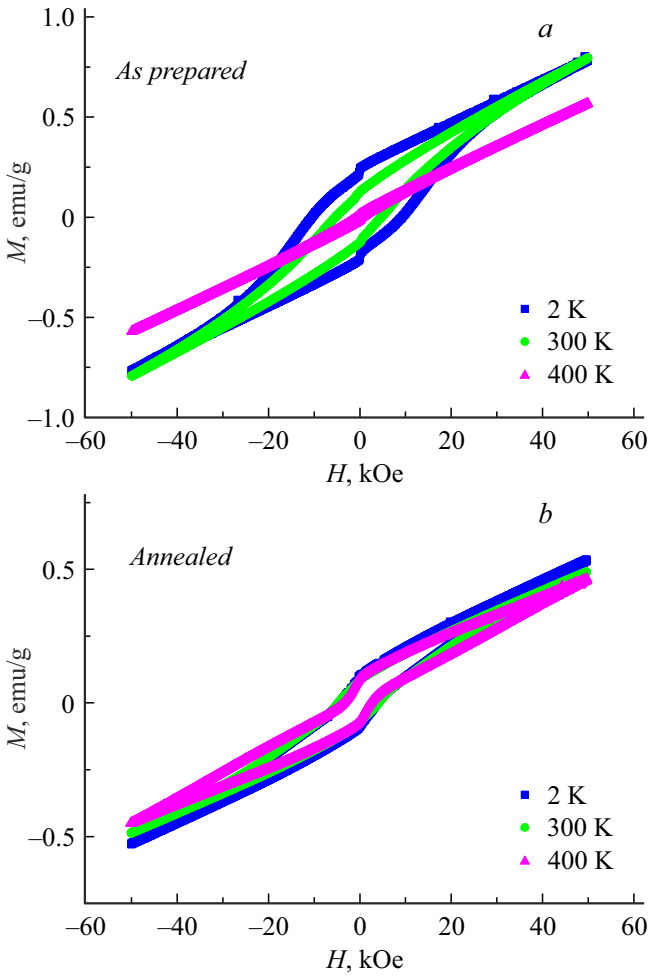

Figure 2. Dependences of magnetization on magnetic field strength $M(H)$ in the form of hysteresis loops at different temperatures of polycrystalline samples of substituted lanthanum-strontium ferrite $La_{0.67}Sr_{0.33}FeO_{3-\delta}$ before (a) and after (b) vacuum heat treatment.

to an internal energy barrier through which it can thermally diffuse in applied fields smaller than those corresponding to the height of the barrier. The sinusoidal nature of the barrier leads to an inversely proportional dependence, similar to the Peierls–Nabarro potential in lattice dislocations and arising - due to the narrowness of the domain walls. The reason that the inversely proportional dependence does not describe the experimental points at all is probably that this model assumes a homogeneous lattice and uses the approximation of a micromagnetic continuum, rather than a discrete spin model, which perhaps should be used when the thickness of the domain wall approaches a value of the order of atomic distance [22].

2. A more complex dependency of the form

$$H_C(T) \sim \{-\nu T \sim (1 + (\nu T)^2)^{1/2}\},$$

where ν is the activation parameter of the domain wall motion previously observed in permanent magnets $Sm_2Co_{17}-SmCo5$ [22–24]. The reason that this dependence does not describe the experimental points at all is probably that this model is valid only for magnetically soft materials, which, judging by the magnitude of the coercive force, does not correspond to the substituted lanthanum-strontium ferrite $La_{0.67}Sr_{0.33}FeO_{3-\delta}$.

3. Exponential dependence of the coercive force on temperature $H_C(T) \sim \exp(-\alpha T)$, previously observed in amorphous alloys $Hf_{57}Fe_{43}$, as in some other materials FeSm, FeZr, $Dy_{60}Fe_{40}$, $(Gd_{1-x}Tb_x)_2Cu$ [25]. The exponential dependence is obtained by taking into account fluctuations in the local values of the anisotropy constant and the wide distribution of energy barriers caused by inhomogeneities in the sample. The parameter α takes into account the amplitude of the inhomogeneities, their period, and the strength of the interaction of the domain wall with the defects.

4. Temperature dependence of the coercive force of the form $H_C(T) \sim 1 - \eta T^{1/2}$, where η is a constant independent of temperature, which is a measure of the ease with which propagation of a thermally activated domain wall can occur [22,23,26]. This dependence has been observed previously, for example, in nanoparticles $Co_xFe_{3-x}O_4$ and alloys $SmCo_{5-x}Ni_x$. The discrepancy with the experiment in this case may be due to the fact that the latter expression works particularly well in those magnets where the anisotropy decreases rapidly with temperature. This, as will be shown later, does not quite correspond to our case.

In initial samples, the drop of H_C with an increase in temperature T occurs quickly enough, so that at 400 K the coercive force barely exceeds zero. An increase in temperature from 2 to 400 K leads to a twenty-five-fold decrease of H_C. At the same time, the coercive force changes little in the annealed samples. Here, an increase in temperature from 2 to 400 K leads to a decrease in H_C by less than one and a half times. The source of coercivity

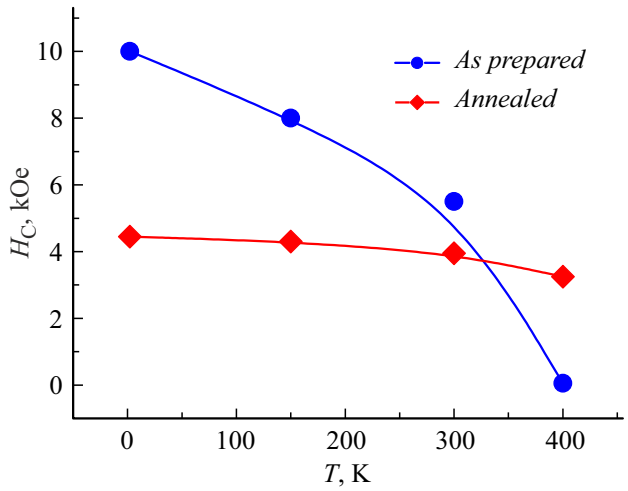

Figure 3. Temperature dependences of the coercive force $H_C(T)$ polycrystalline samples of substituted lanthanum-strontium ferrite $La_{0.67}Sr_{0.33}FeO_{3-\delta}$ before (blue symbols) and after (red symbols) vacuum heat treatment. Solid lines show the spline.

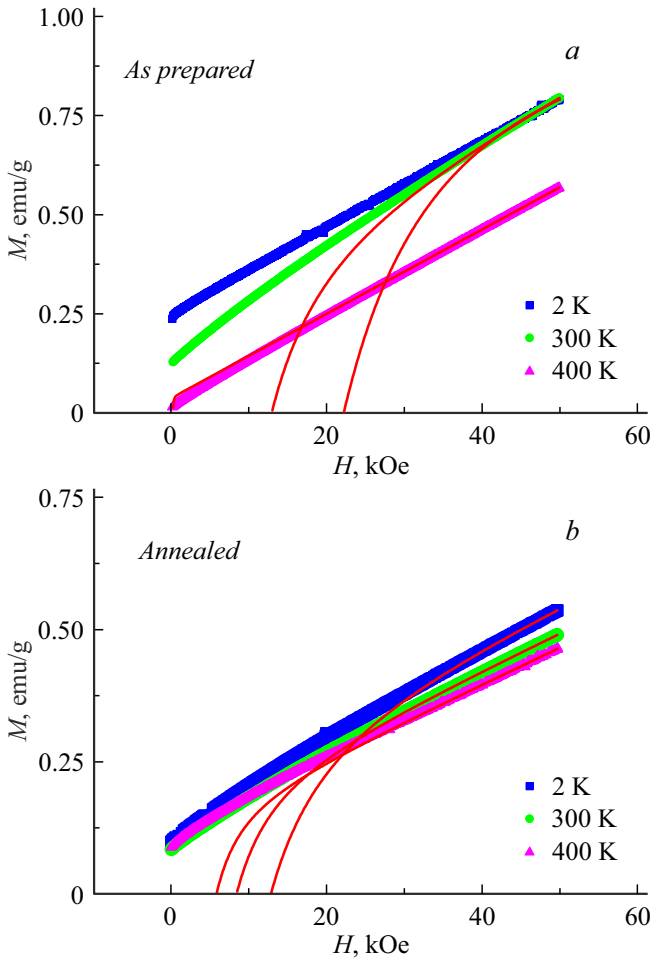

Figure 4. Dependences of magnetization on magnetic field strength $M(H)$ at different temperatures of polycrystalline samples of substituted lanthanum-strontium ferrite $La_{0.67}Sr_{0.33}FeO_{3-\delta}$ before (a) and after (b) vacuum heat treatment. Solid red lines show approximations (explanations in the text).

is magnetic anisotropy, expressed either by the anisotropy field H_A or by the magnetic anisotropy constant K. In many ways, magnetic hysteresis is also determined by a structural factor, which is expressed in the different dynamics of the movement of domain walls in the field of extended structural defects. The temperature variations H_C in each of the samples are due only to the first factor, the temperature dependence of the magnetic anisotropy, since the structure remains fixed. The almost twofold reduction in coercive force caused by vacuum heat treatment may be due to both factors, i.e. both by attenuation of magnetic anisotropy and by structural variations occurring during annealing. Below we will consider each of the two factors separately. To discuss the first factor, it is necessary to determine the anisotropy field HA (anisotropy constant K) and their temperature variations in each of the two samples. To do this, we will analyze and process the magnetization curves $M(H)$.

In the region of strong magnetic fields, as the magnetization approaches MS saturation, the latter depends on H according to the power law $M(H) = M_S(1 - (H_A/H)^2) + \chi H$ [25]. This expression approximated the high-field $H > 40$ kOe experimental dependences $M(H)$ with extrapolation of the magnetization to $H = 0$ for visual visualization of the field H_A (red lines are shown in Fig. 4). From the approximation, the values of the magnetic anisotropy field H_A and saturation magnetization M_S for each temperature were determined, which, according to the expression $H_A = 2K/M_S$, in turn were recalculated into the values of the magnetic anisotropy constant K. The temperature variations of M_S and K are shown in Fig. 5. Let's first discuss the dependencies $M_S(T)$ and $K(T)$, then the effect of vacuum heat treatment on them.

As can be seen from Fig. 5, a, the temperature dependences of saturation magnetization $M_S(T)$ of polycrystalline samples of substituted lanthanum-strontium fer-

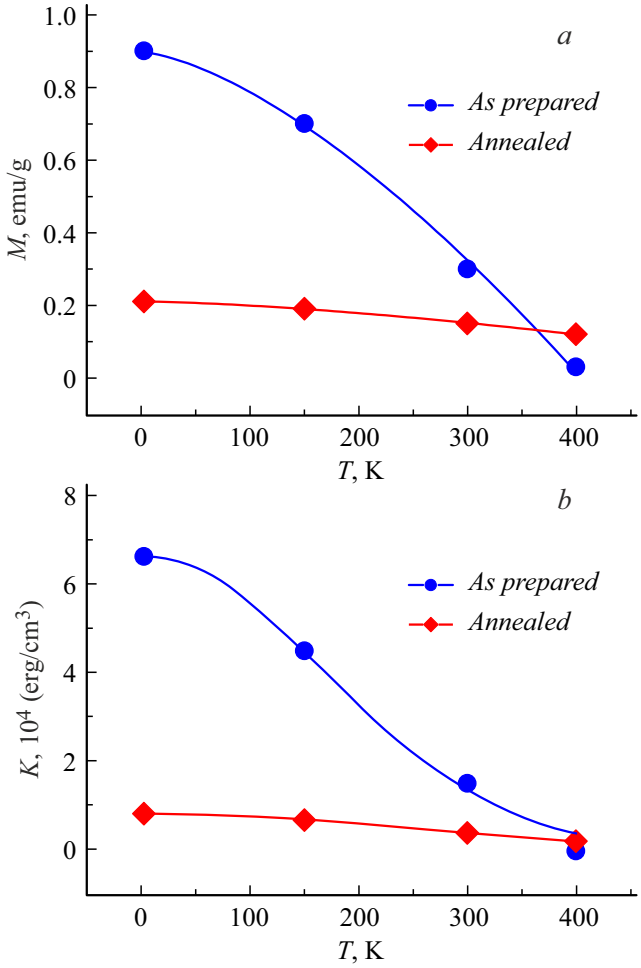

Figure 5. Temperature dependences of saturation magnetization $M_S(T)$ (a) and magnetic anisotropy constants $K(T)$ (b) of polycrystalline samples of substituted lanthanum-strontium ferrite $La_{0.67}Sr_{0.33}FeO_{3-\delta}$ before (blue symbols) and after (red symbols) vacuum heat treatment. Solid lines show approximations (explanations in the text).

rite $La_{0.67}Sr_{0.33}FeO_{3-\delta}$ as before, and after vacuum heat treatment are described with high accuracy by Bloch 's law (law 3/2) $M_S(T) = M_{S0}(1 - (T/T_N)^{3/2})$ [24]. In the initial samples, the saturation magnetization at $T \to 0$ $M_{S0} = 0.9$ emu/g, and the critical temperature of magnetic ordering (the Neel temperature in this case) $T_N = 397$ K. In annealed samples M_{S0} has the value 0.2 emu/g, Curie temperature is $T_N = 605$ K. Thus, vacuum annealing, on the one hand, causes an almost fivefold decrease in saturation magnetization, on the other hand, an almost twofold increase in Nickel temperature. Both effects are consistently explained by increased antiferromagnetic exchange in the samples as a result of vacuum heat treatment. Mathematically, this is expressed in an increase in the value of the exchange integral J_{EX} (the exchange field $H_{EX} = zSJ_{EX}/g\mu_B$). In the last expression for the exchange field $z = 6$ is the number of nearest neighbors, $S = 5/2$ and $g = 2$ is ion spin and g-iron factor Fe^{3+}, μ_B is Boron magneton.

Let's use the well-known relationship between J_{EX} and T_N, expressed by the formula $T_N = zS(S+1)J_{EX}/3k_B$, where k_B is the Boltzmann constant [27]. The latter expression, knowing T_N, allows directly estimating the values of the exchange integrals J_{EX} for samples before and after vacuum heat treatment. In initial samples $J_{EX} = 32$ K, in annealed samples, respectively, one and a half times more: $J_{EX} = 49$ K. The resulting exchange integral J_{EX} is an additive physical quantity, and is a linear combination of antiferromagnetic (J_{AF}) and ferromagnetic (J_F) components of the exchange interaction. Changes in the crystal structure of $La_{1-x}Sc_xFeO_{3-\delta}$ during vacuum heat treatment, among other things, always lead to an increase of angle θ of bond $Fe^{3+}O^2 - Fe^{3+}$ [28]. The hyperexchange antiferromagnetic interaction increases with increasing θ — according to the expression $J_{AF}(\theta) = A + B \cdot \cos\theta + C \cdot \cos^2\theta$ [27]. As can be seen from the last expression, the overexchange integral JAF reaches a maximum at $\theta = 180°$. In addition to strengthening the antiferromagnetic exchange channel in $Fe^{3+}-Fe^{3+}$ pairs, vacuum heat treatment weakens the ferromagnetic channel in $Fe^{3+}-Fe^{4+}$ pairs, which is realized by the mechanism of double Zener exchange due to the removal of Fe^{4+} ions from the crystal lattice. The increase of J_{AF} with simultaneous attenuation of J_F leads to an increase in J_{EX} and a corresponding increase in the temperature of the gel T_N as a result of vacuum heat treatment. In conclusion of this part of this work, we note that we have determined the values of the exchange field H_{EX} according to the above formula for samples before and after vacuum heat treatment. In initial samples $H_{EX} = 2460$ kOe, it is one and a half times greater in annealed samples, respectively: $H_{EX} = 3770$ kOe. Knowledge of the magnitude of the exchange field H_{EX} is not important in itself, but will be needed for the subsequent discussion of the decrease in saturation magnetization caused by vacuum annealing.

The magnetization of a weak ferromagnet depends on the ratio of the contributions of the isotropic exchange interaction (H_{EX}) and the antisymmetric exchange interaction of the Dzyaloshinskii–Moriya (H_D) into the total effective exchange and is determined by the expression $M_{Fe}H_D/2H_{EX}$ [29]. Here $M_{Fe} = 2gS\mu_B/\rho V = 60$ emu/g is the magnetization of one of the sublattices of the beveled antiferromagnet [27]. The factor $H_D/2H_{EX}$ determines the value of the angle of bevel of the sublattices according to the expression $\sin\varphi = (H_D + H)/2H_{EX}$ [29]. As stated above, vacuum annealing causes an almost fivefold decrease in magnetization. This means that the bevel angle φ decreases as a result of vacuum heat treatment. On the one hand, this occurs, as was established above, due to an increase in the exchange field H_{EX} caused by an increase in the bond angle Fe–O–Fe due to annealing. On the other hand, variations of the Dzyaloshinskii field H_D initiated by him cannot be excluded, since the latter depends both on the angle of the superexchange bond and on its spatial orientation, which is rearranged by annealing.

As can be seen from Fig. 5, *b*, the temperature dependences of the magnetic anisotropy constants $K(T)$ of polycrystalline samples of substituted lanthanum-strontium ferrite $La_{0.67}Sr_{0.33}FeO_{3-\delta}$ as both before and after vacuum heat treatment are described with high accuracy by Bryukhatov–Kirensky empirical expression $K(T) = K_0 \exp(-\beta T^2)$ [26]. The parameter determining the temperature course, $\beta = 2 \cdot 10^{-5}$ K^{-2} in initial samples, the magnetic anisotropy constant at $T \to 0$ K $K_0 = 7 \cdot 10^4$ erg/cm^3. In annealed samples, K_0 takes the value $8 \cdot 10^3$ erg/cm^3, $\beta = 9 \cdot 10^{-6}$ K^{-2}. Thus, vacuum annealing, on the one hand, causes a weakening of the magnetic anisotropy by almost an order of magnitude, on the other hand, weakens its dependence on temperature. We will discuss each of the effects separately below.

The magnetic anisotropy of substituted lanthanum ferrite–strontium $La_{1-x}Sc_xFeO_{3-\delta}$ results mainly from the one-ionic anisotropy of ions Fe^{3+} and Fe^{4+} (magnetocrystalline anisotropy). The following one-electron Hamiltonian is usually used to simulate the effect of the crystal structure on the magnetic anisotropy of ions Fe^{3+} and Fe^{4+}: $H = V_{CF}(D) + \xi LS - J_{EX}S\hat{a}$ [30]. The first term $V_{CF}(D)$ is a matrix that takes into account the influence of the crystal field on the orbital states of the ions Fe^{3+} and Fe^{4+}. The parameter $V_{CF}(D)$ reflects the distortion of octahedra FeO_6 in orthorhombic substituted lanthanum-strontium ferrite $La_{0.67}Sr_{0.33}FeO_{3-\delta}$, resulting in the different length of bond Fe–O along the directions a, b and c. The distortions are described in terms of the crystal field potential V_{CF}, which depends on the perturbation parameter D, which is proportional to the displacement of ions Fe^{3+}, Fe^{4+} and O^{2-}. The second term $\xi\mathbf{LS}$ defines the spin-orbit interaction, depending on the constant spin-orbit bond ξ, as well as on the orbital **L** and spin **S** moments. The third term $J_{EX}\mathbf{S}\hat{\mathbf{a}}$ is an exchange interaction between ions Fe^{3+} and Fe^{4+}, determined by the molecular exchange field $J_{EX}\hat{\mathbf{a}}$ acting on a given spin from all other spins. Diagonalization of the Hamiltonian H allows us to find the energy of magnetic anisotropy $E_A = \xi^2 D/E_{EXCF}^2$, depending on the crystal

field, structural distortions, spin-orbit interaction and the molecular exchange field. Here E_{EXCF} is the characteristic energy scale of the effects of the crystal field and exchange interactions. Let's discuss the possible effect of vacuum heat treatment on each of the parameters included in the last expression for E_A. First-, as was shown in the works of [19,20] and already mentioned above, vacuum annealing is accompanied by a decrease in the distortion of the crystal lattice, which means the parameter D. Secondly-, an increase in antiferromagnetic exchange in samples as a result of vacuum heat treatment is naturally reflected in an increase in E_{EXCF}. In -third, the spin-orbit bond constant ξ in Fe^{4+} ions exceeds that in Fe^{3+} ions [31,32]. Therefore, the removal of Fe^{4+} ions from the crystal lattice caused by vacuum annealing leads to a weakening of the spin-orbit interaction. As follows from the expression for the energy of magnetic anisotropy, all three factors considered simultaneously as a result of vacuum heat treatment decrease the value of E_A and, accordingly, the value of the anisotropy constant K in exact agreement with the experiment described above.

The weakening of the $K(T)$ dependence as a result of vacuum heat treatment is explained within the framework of the general law of temperature dependence of magnetic anisotropy constants (law of degree $l(l+1)/2$) $K(T)/K_0 = [M_S(T)/M_{S0}]^{l(l+1)/2}$. The parameter l, which is equal to 1, 2, 3, etc., corresponds to the order of decomposition of the energy of magnetic anisotropy according to the degrees of the guiding cosines of the magnetization vector relative to the main crystallographic axes [33]. Fig. 6 shows the dependences of the normalized magnetic anisotropy constant K/K_0 on the normalized saturation magnetization M_S/M_{S0} in polycrystalline samples of substituted lanthanum ferrite–strontium $La_{0.67}Sr_{0.33}FeO_{3-\delta}$ before and after vacuum heat treatment. The alignment of these dependencies indicates that in both cases $l = 1$. This indicates that the main contribution to the effective constant K is made by the anisotropy constant of the first order. The weakening of the dependence $K(T)$ (Fig. 5, *b*) and, accordingly, the coercive force $H_C(T)$ (Fig. 2) during vacuum annealing is explained by the formation of a smoother temperature course as a result of annealing $M_S(T)$ (fig. 5, *a*).

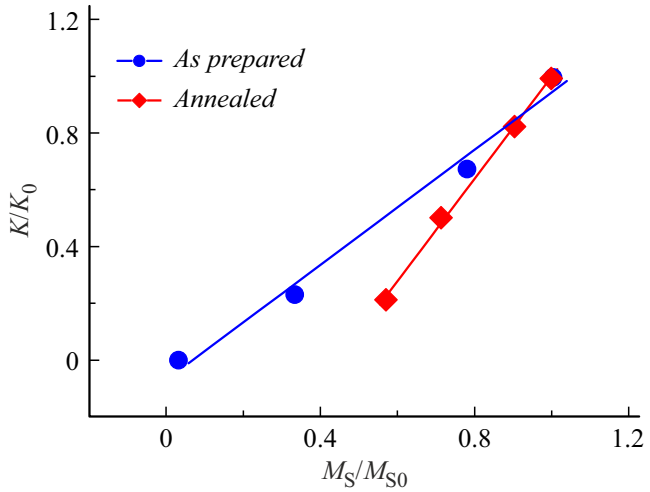

Figure 6. Dependences of the normalized magnetic anisotropy constant K/K_0 on the normalized saturation magnetization M_S/M_{S0} in polycrystalline samples of substituted lanthanum-strontium ferrite $La_{0.67}Sr_{0.33}FeO_{3-\delta}$ to (blue symbols) and after (red symbols) vacuum heat treatment. Solid lines show approximations (explanations in the text).

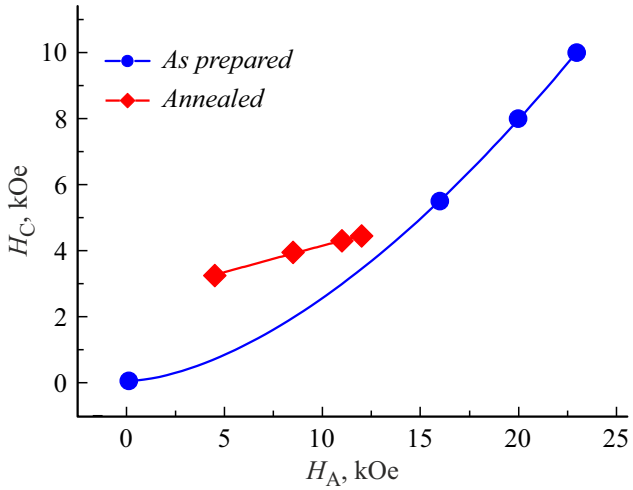

Figure 7. Dependences of the coercive force on the magnetic anisotropy field $H_C(H_A)$ polycrystalline samples of substituted lanthanum-strontium ferrite $La_{0.67}Sr_{0.33}FeO_{3-\delta}$ before (blue symbols) and after (red symbols) vacuum heat treatment. Solid lines show approximations (explanations in the text).

The most complete and complete theory of the temperature dependence of the coercive force was constructed by Kronmuller [24]. According to it, $H_C(T) \sim (K/M_S)^d$, where d is an exponent depending on the microscopic mechanism of magnetic hysteresis formation. If the hysteresis is caused by the fixation of the domain walls on extended defects, then two cases are possible. The dependence $H_C(T) \sim (K/M_S)^{3/2}$ corresponds to small defects smaller than the thickness of the domain wall. For large defects, the dependence $H_C(T) \sim K/M_S$ corresponds to the thickness of the domain wall. That is, in both cases, the coercive force is proportional to the degree of the magnetic anisotropy field H_A. Thus, to answer the question about the nature of magnetic hysteresis in the considered substituted lanthanum-strontium ferrites $La_{1-x}Sc_xFeO_{3-\delta}$, we constructed dependences of the coercive force on the magnetic anisotropy field $H_C(H_A)$ before and after vacuum heat treatment (Fig. 7). In the initial samples, the dependence of the coercive force H_C on the anisotropy field H_A is described by a power function with exponent $d = 1.6 \pm 0.1$ (Fig. 7). This means that the microscopic mechanism responsible for the formation of magnetic hysteresis in them is the fixation of domain walls on small defects, the dimensions of which are smaller than the thickness of the domain wall. In annealed samples, the dependence of the coercive force H_C on the anisotropy field H_A is described by a

power function with the exponent $d = 0.9 \pm 0.1$ (Fig. 7). This means that the microscopic mechanism responsible for the formation of magnetic hysteresis in them is the fixation of domain walls on large defects, the dimensions of which are larger than the thickness of the domain wall. In polycrystals, grain boundaries are the most significant extended defects which are pinning centers of domain walls. Therefore, variations in the dependence $H_C(H_A)$ caused by vacuum heat treatment can naturally be attributed to changes in the defective structure and state of the grain boundaries.

Conclusion

A vibration magnetometer was used to measure the dependences of the magnetic moment on the magnetic field strength $M(H)$ in the form of hysteresis loops over a wide temperature range of polycrystalline samples of substituted lanthanum-strontium ferrite $La_{1-x}Sc_xFeO_{3-\delta}$ before and after vacuum heat treatment. The shape of the magnetic hysteresis loops in both cases is typical for weak ferromagnets and inherits the shape of the curves $M(H)$ of both antiferromagnets and ferromagnets. The antiferromagnetic component is manifested in relatively strong magnetic fields, where the dependence $M(H)$ is linear. The ferromagnetic component manifests itself in relatively weak magnetic fields, and demonstrates quite significant hysteresis and a tendency to saturation.

The temperature dependences of the coercive force $H_C(T)$ of the samples before and after vacuum heat treatment were determined. The increase in temperature in the samples of both series leads to a narrowing of the magnetic hysteresis loop, but the curves $H_C(T)$ are not described by any known empirical expression. The coercive force HC in the initial samples reaches 10 kOe at $T = 2$ K. The drop of H_C with an increase of T occurs quickly enough, so that the coercive force barely exceeds zero at 400 K. Vacuum heat treatment causes a decrease in the coercive force, so that in annealed samples H_C it does not reach 5 kOe at $T = 2$ K. At the same time, in annealed samples, the coercive force hardly changes with temperature.

Approximation of the dependences $M(H)$ of the samples before and after vacuum heat treatment by the well-known law of approximation to saturation allowed us to establish the values of the magnetic anisotropy field H_A and saturation magnetization M_S for each temperature, which, in turn, were recalculated into the values of the magnetic anisotropy constants K.

The temperature dependence of saturation magnetization M_S in both cases is described with high accuracy by Bloch's law (law 3/2). Vacuum annealing, on the one hand, causes a decrease in saturation magnetization from $M_{S0} = 0.9$ to 0.2 emu/g, on the other hand, it results in an increase of the Nickel temperature from T_N=0397 K to T_N=605 K. Both effects are consistently explained by increased antiferromagnetic exchange. The values of the exchange integral J_{EX} and the exchange field H_{EX} are determined. $J_{EX} = 32$ K and $H_{EX} = 2460$ kOe in initial samples, $J_{EX} = 49$ K and $H_{EX} = 3770$ kOe in annealed samples. An increase in $J_{EX}(H_{EX})$ and a corresponding increase in T_N as a result of vacuum heat treatment occurs due to the redistribution of contributions of antiferromagnetic and ferromagnetic components to effective exchange. Experimental evidence has been obtained that vacuum annealing also initiates variations of the Dzyaloshinskii field H_D.

The temperature dependence of the magnetic anisotropy constants K in both cases is described with high accuracy by the empirical Bryukhatov-Kirensky expression. Vacuum annealing, on the one hand, causes a weakening of magnetic anisotropy (in initial samples $K_0 = 7 \cdot 10^4$ erg/cm^3, in annealed samples $K_0 = 8 \cdot 10^3$ erg/cm^3), on the other hand, it weakens its dependence on temperature. The weakening of magnetic anisotropy as a result of vacuum heat treatment is due to the synergistic effect of reducing the distortion of the crystal lattice, enhancing antiferromagnetic exchange and weakening the spin-orbit interaction. The weakening of the $K(T)$ dependence as a result of vacuum heat treatment is explained within the framework of the general law of temperature dependence of magnetic anisotropy constants (law of degree $l(l+1)/2$).

Analysis of the values of the coercive force in coordinates $H_C(H_A)$ within the framework of the Kronmuller theory allowed revealing the microscopic mechanism responsible for the formation of magnetic hysteresis in samples before and after vacuum heat treatment. In the initial samples, this is the fixation of the domain walls on small defects, the dimensions of which are smaller than the thickness of the domain wall. In annealed samples, the domain walls are fixed to large defects, the dimensions of which are greater than the thickness of the domain wall. Variations in the $H_C(H_A)$ dependence caused by vacuum heat treatment are explained by changes in the defective structure and state of the grain boundaries.

Acknowledgments

The authors would like to thank V.D. Sedykh for the samples provided, O.G. Rybchenko for X-ray diffraction studies, and M.V.Zhidkov for assistance in conducting magnetometric studies.

Funding

This study was supported by the Ministry of Science and Higher Education of the Russian Federation under state assignment 124013100858-3.

Conflict of interest

The authors declare that they have no conflict of interest.

References

[1] U.F. Vogt, J. Sfeir, J. Richter, C. Soltmann, P. Holtappels. Pure Appl. Chem., **80** (11), 2543 (2008). DOI: 10.1351/pac200880112543

[2] C.O. Augustin, R. Kalai, R. Nagaraj, L.J. Berchmans. Mater. Chem. Phys., **89** (2-3), 406 (2005). DOI: 10.1016/j.matchemphys.2004.09.028

[3] M. Søgaard, P.V. Hendriksen, M. Mogensen. J. Solid State Chem., **180** (4), 1489 (2007). DOI: 10.1016/j.jssc.2007.02.012

[4] M.V. Patrakeev, J.A. Bahteeva, E.B. Mitberg, I.A. Leonidov, V.L. Kozhevnikov, K.R. Poeppelmeier. J. Solid State Chem., **172** (1), 219 (2003). DOI: 10.1016/S0022-4596(03)00040-9

[5] H. Liu, H. Fan, X. Xu, H. Lu, T. Zhang. Solid State Electron., **79**, 87 (2013). DOI: 10.1016/j.sse.2012.07.004

[6] A. Wattiaux, J. C. Grenier, M. Pouchard, P. Hagenmuller. J. Electrochem. Soc., **134**, 1718 (1987). DOI: 10.1149/1.2100742

[7] J. Li, X. Kou, Y. Qin, H. He. Phys. Stat. Sol., **191** (1), 255 (2002). DOI: 10.1002/1521-396x(200205)191:1¡255::aid-pssa255¿3.0.co;2-n

[8] A.H. Bobeck. Bell Syst. Tech. J., **46** (8), 1901 (1967). DOI: 10.1002/j.1538-7305.1967.tb03177.x

[9] A. Goldman. *Modern Ferrite Technology* (Springer, NY., 2006), DOI: 10.1007/978-0-387-29413-1

[10] D.W. Richerson, W.E. Lee. *Modern Ceramic Engineering: Properties, Processes and Use in Design* (CRC Press, Boca Raton, 2018), DOI: 10.1201/9780429488245

[11] I.N. Sora, F. Fontana, R. Passalacqua, C. Ampelli, S. Perathoner, G. Centi, F. Parrino, L. Palmisano. Electrochim. Acta, **109** (30), 710 (2013). DOI: 10.1016/j.electacta.2013.07.132

[12] J.R. Hayes, A.P. Grosvenor. J. Phys.: Condens. Matter, **23** (46), 465502 (2011). DOI: 10.1088/0953-8984/23/46/465502

[13] M. Popa, J.M.C. Moreno. J. Alloys Compd., **509** (10), 4108 (2011). DOI: 10.1016/j.jallcom.2010.12.162

[14] H. Wu, Z. Xia, X. Zhang, S. Huang, Me. Wei, Fe. Yang, Y. Song, G. Xiao, Z. Ouyang, Z. Wang. Ceram. Int., **44** (1), 146 (2018). DOI: 10.1016/j.ceramint.2017.09.150

[15] L. Huang, L. Cheng, S. Pan, Y. He, C. Tian, J. Yu, H. Zhou. Ceram. Int., **46** (17), 27352 (2018). DOI: 10.1016/j.ceramint.2020.07.220

[16] F. Yang, X.X. Yang, Q. Lin, R.J. Wang, H. Yang, Y. He. Mater. Sci., **25** (3), 231 (2019). DOI: 10.5755/j01.ms.25.3.19455

[17] R.B. da Silva, J.M. Soares, J.A.P. da Costa, J.H. de Araújo, A.R. Rodrigues, F.L.A. Machado. J. Magn. Magn. Mater., **466** (15), 306 (2018). DOI: 10.1016/j.jmmm.2018.07.040

[18] F. Gao, P.L. Li, Y.Y. Weng, S. Dong, L.F. Wang, L.Y. Lv, K.F. Wang, J.-M. Liu, Z.F. Ren. Appl. Phys. Lett., **91** (7), 072504 (2007). DOI: 10.1063/1.2768895

[19] V. Sedykh, O. Rybchenko, V. Rusakov, S. Zaitsev, O. Barkalov, E. Postnova, T. Gubaidulina, D. Pchelina, V. Kulakov. J. Phys. Chem. Solids, **171**, 111001 (2022). DOI: 10.1016/j.jpcs.2022.111001

[20] V.D. Sedykh, V.S. Rusakov, T.V. Gubaidulina. Phys. Solid State, **65** (4), 613 (2023). DOI: 10.21883/PSS.2023.04.56003.18

[21] A. Enders, D. Repetto, D. Peterka, K. Kern. Phys. Rev. B, **72** (5), 054446 (2005). DOI: 10.1103/PhysRevB.72.054446

[22] H. Oesterreicher, F.T. Parker, M. Misroch. Phys. Rev. B, **18** (1), 480 (1978). DOI: 10.1103/PhysRevB.18.480

[23] K.-D. Durst, H. Kronmüller, F.T. Parker, H. Oesterreicher. Phys. Status Solidi A, **95** (1), 213 (1986). DOI: 10.1002/pssa.2210950127

[24] R. Kütterer, H.-R. Hilzinger, H. Kronmüller. J. Magn. Magn. Mater., **4** (1-4), 1 (1977). DOI: 10.1016/0304-8853(77)90004-X

[25] D. Pajić, K. Zadro, R. Ristić, I. Živković, Ž. Skoko, E. Babić. J. Phys.: Condens. Matter, **19** (29), 296207 (2007). DOI: 10.1088/0953-8984/19/29/296207

[26] T.E. Torres. E. Lima, A. Mayoral. A. Ibarra. C. Marquina. M.R. Ibarra. G.F. Goya. J. Appl. Phys., **118** (18), 183902 (2015). DOI: 10.1063/1.4935146

[27] A. Moskvin. Magnetochem., **7** (8), 111 (2021). DOI: 10.3390/magnetochemistry7080111

[28] J.B. Yang, W.B. Yelon, W.J. James, Z. Chu, M. Kornecki, Y.X. Xie, X.D. Zhou, H.U. Anderson, A.G. Joshi, S.K. Malik. Phys. Rev. B, **66** (18), 184415 (2002). DOI: 10.1103/PhysRevB.66.184415

[29] E.A. Turov. Sov. Phys. JETP, **36** (9), 890 (1959). http://www.jetp.ras.ru/cgi-bin/dn/e_009_04_0890.pdf

[30] S. Cao, X. Zhang, T.R. Paudel, K. Sinha, X. Wang, X. Jiang, W. Wang, S. Brutsche, J. Wang, P.J. Ryan, J.-W. Kim, X. Cheng, E.Y. Tsymbal, P.A. Dowben, X. Xu. J. Condens. Matter Phys., **28** (15), 156001 (2016). DOI: 10.1088/0953-8984/28/15/156001

[31] G.M. Cole, B.B. Garrett. Inorg. Chem., **9** (8), 1898 (1970). DOI: 10.1021/ic50090a020

[32] R. Al-Mobarak, K.D. Warren. Chem. Phys. Lett., **21** (3), 513 (1973). DOI: 10.1016/0009-2614(73)80296-9

[33] S. Krupička. *Physik der Ferrite und der verwandten magnetischen Oxide* (Springer, Wiesbaden, 1973), DOI: 10.1007/978-3-322-83522-2

Translated by A.Akhtyamov